JOURNAL OF MAGNETIC RESONANCE IMAGING 15:315–323 (2002)
DOI 10.1002/jmri.10074

Original Research

Effect of IL-1β-Induced Macromolecular Depletion on Residual Quadrupolar Interaction in Articular Cartilage

Arijitt Borthakur, PhD,[1]* Erik M. Shapiro, PhD,[2] Jennifer Beers, MA,[1]
Sagar Kudchodkar, BS,[1] J. Bruce Kneeland, MD,[1] and Ravinder Reddy, PhD[1]

Purpose: Sodium multiple-quantum filtered (MQF) NMR spectroscopy may potentially be used to measure proteoglycan (PG) depletion in cartilage caused by osteoarthritis (OA). The purpose of this work was to quantify the effect of interleukin-1 (IL-1β)-induced macromolecule depletion on the residual quadrupolar interaction (RQI) of sodium in bovine cartilage plugs.

Materials and Methods: Fifteen 8-mm-diameter cartilage plug specimens were cored from the articular surface of fresh bovine patellae. All plugs were kept in culture media and nine of the plugs were subjected to interleukin-1 (IL-1β)-induced degeneration of cartilage for 4, 6, and 7 days. Sodium NMR spectra were obtained from each sample with a 1-cm-diameter solenoid coil in a 2T whole-body magnet interfaced to a custom-built spectrometer. We employed a previously described theoretical model to analyze triple-quantum filtered (TQF) and double-quantum filtered magic angle (DQFMA) spectra obtained from normal cartilage and cartilage treated with IL-1β. The model assumes a static Gaussian distribution of the RQI frequency, ω_Q, in the sample. TQF and DQFMA spectra from each sample were fitted with the appropriate signal expressions to determine σ (the root mean square (RMS) ω_Q), T_{2f}, and T_{2s}. An inversion-recovery sequence was used to determine T_1 of each plug. A spectrophotometric assay was used to determine the amount of PG depleted from each plug. Histology was performed to visualize the PG loss in cartilage plugs. We defined σ as the measure of changes in macroscopic order in the tissue.

Results: Simulated spectra from the theoretical model were in excellent agreement with the experimental data. We were able to determine the relaxation times as well as σ of each specimen from their corresponding fits. T_{2f} ranged between 2.26–3.50 msec, decreasing with increased PG loss. Over the range of PG depletion investigated, T_{2s} increased from 12.3 msec to 14.9 msec, and T_1 increased from 16 msec to 21 msec, while σ decreased from 180 Hz to 120 Hz. The order of macromolecules in the cartilage tissue decreased substantially with PG loss. Histology sections clearly showed qualitative visualization of the PG loss in cartilage following treatment with IL-1β.

Conclusion: We demonstrated that IL-β-induced macromolecule depletion in cartilage not only changes the relaxation characteristics of sodium but also changes RQI of the tissue. Using MQF sodium spectroscopy we quantified the changes in σ and showed that loss of macromolecules reduces the degree of order in the tissue.

Key Words: sodium; NMR; multiple-quantum filter; cartilage; proteoglycans
J. Magn. Reson. Imaging 2002;15:315–323.

THE EARLY STAGE OF OSTEOARTHRITIS (OA) is associated with the preferential loss of proteoglycans (PGs) from the extracellular matrix (ECM) of cartilage (1,2). PGs maintain a fixed negative charge in the ECM and attract sodium ions and water molecules. PG loss is associated with a loss of sodium in cartilage (3). Recently it was shown (4–7) that sodium NMR can be used to measure the PG content of cartilage.

In cartilage, sodium ions are in a slow motion regime ($\omega_O\tau_C \sim 1$, where ω_O is the Larmor precession frequency and τ_C is the correlation time), which results in biexponential relaxation rates (8). Furthermore, cartilage, like most biological tissues, is heterogeneous in nature. However, some order exists at the local level. This ordering is primarily due to the anisotropic arrangement of collagen fibril bundles, PG, and other macromolecules in the ECM. The ordering in the ECM in cartilage produces a non-zero electric field gradient (EFG). The interaction of this EFG with quadrupolar nuclei, like ^{23}Na, results in a residual quadrupolar interaction (RQI). The quadrupolar interaction is dependent on the orientation of the EFG to the external static magnetic field, B_0. Recently, the presence of RQI in cartilage was demonstrated by sodium multiple-quantum filtered

[1]Department of Radiology, University of Pennsylvania, Philadelphia, Pennsylvania.
[2]Department of Chemistry, University of Pennsylvania, Philadelphia, Pennsylvania.
Contract grant sponsor: NIH; Contract grant number: RR02305; Contract grant sponsor: National Institutes of Arthritis, Musculoskeletal, and Skin Diseases (NIAMS); Contract grant numbers: R01-AR45242; R01-AR45404.
*Address reprint requests to: A.B., Department of Radiology, University of Pennsylvania, B1 Stellar-Chance Laboratories, 422 Curie Boulevard, Philadelphia, PA 19104-6100.
E-mail: ari@mail.mmrrcc.upenn.edu
Received May 24, 2001; Accepted November 16, 2001.

(MQF) NMR spectroscopy (9). The magnitude of quadrupolar interaction frequency (ω_Q) represents the degree of order of the macromolecules in the tissue. Hence it is possible to probe this parameter, which in turn may provide information about the structural integrity of biological tissues. Sodium MQF-NMR spectroscopy and imaging of biological tissues have been performed both in vivo (10–12) and in vitro (8,9,13,14). MQF-NMR spectroscopy is uniquely suited for measuring ω_Q, as well as biexponential relaxation times.

It was previously shown (15), using isolated model systems of cartilage ECM components, that the contribution to RQI in cartilage is due to ordering of collagen bundles and that PG does not contribute to the RQI. Although these were meticulous studies, since they were performed on isolated collagen and PG molecules, it is difficult to determine the effects of PG on the RQI in the presence of collagen in intact cartilage. This can only be accomplished by selective depletion of PG from cartilage using an appropriate enzyme or cytokine. Interleukin-1 (IL-1β) is a cytokine that enhances formation of metalloproteinases by chondrocytes. Proteinases are responsible for PG depletion in cartilage both in vivo (16,17) and in vitro (18,19). An increased level of IL-1β has been observed in the early stages of OA (20). It was shown previously (21) that sodium relaxation rates change with IL-1β-induced cartilage degeneration. However, this simplistic model did not incorporate ω_Q into the calculations.

In this work, we investigated the effect of degradation of the ECM of articular cartilage with IL-1β on ω_Q, the short (T_{2f}) and long (T_{2s}) components of the transverse relaxation time, as well as the longitudinal relaxation time (T_1) of sodium. The magnitude of σ (the RMS ω_Q) was used as a measure of the ordering of macromolecules in the tissue. We demonstrated that the macromolecule depletion induced by IL-1β resulted in changes in the local order of the ECM, which was reflected not only in the relaxation times but also in the σ.

THEORY

The spin dynamics of quadrupolar nuclei, in biological tissues, can be determined by forming the appropriate interaction Hamiltonian and computing the response to a given pulse sequence. The Hamiltonian for the combined Zeeman interaction and a much smaller quadrupolar interaction can be expressed as:

$$\hat{\boldsymbol{H}} = \hat{\boldsymbol{H}}_Z + \hat{\boldsymbol{H}}_Q \qquad (1)$$

Where

$$\hat{\boldsymbol{H}}_Z = -\gamma\hbar B_O \hat{\boldsymbol{I}}_Z \qquad (2)$$

and

$$\hat{\boldsymbol{H}}_Q = \frac{e^2qQ}{24}(3\cos^2\theta - 1 + \eta\sin^2\theta\cos 2\phi)\left(3\hat{\boldsymbol{I}}_Z^2 - \frac{15}{4}\right) \qquad (3)$$

Where $\hat{I}_Z$ is the nuclear spin angular momentum operator, eQ is the nuclear quadrupole moment, and eq is the principal value of the residual EFG along its major axis. Angles θ and ϕ are the polar and azimuthal angles, respectively, between the orientation of the EFG and the static magnetic field, B_0, and η is the asymmetry parameter of the EFG.

Several models have been used to analyze MQF-NMR spectra of spin-3/2 in biological systems (14). Eliav and Navon (15) showed that a model that assumes a Gaussian-weighted distribution of ω_Q values provided the best fit for the MQF-NMR signal from fresh bovine nasal cartilage. This model provided the best fit for Jeener-Broekaert spectra obtained from bovine articular cartilage as well (22). In the present investigation, we used a similar model that assumes a static Gaussian distribution of ω_Q to describe the sodium MQF-NMR signal from bovine cartilage (23,24). In this model, the tissue is comprised of several volumes called "domains." The average volume of the domain is greater than the average volume traversed by a diffusing sodium ion within its coherence lifetime. Within each domain, the macromolecules are nonrandomly arranged and interact anisotropically with fluid and hydrated ions. As a result there exists a residual EFG, of magnitude eq and direction that is determined by the orientation of the domain and the asymmetry parameter. Each domain has a quadrupolar interaction frequency, ω_Q, given by:

$$\omega_Q = \frac{\pi}{2}\cdot\frac{e^2qQ}{\hbar}(3\cos^2\theta - 1 + \eta\sin^2\theta\cos 2\phi) \qquad (4)$$

If the sample is a liquid crystal, where all the domains have the same residual EFG and are oriented parallel to each other, we expect an NMR spectrum with three narrow lines. A random orientation of the EFG in the different domains will result in a Pake powder pattern NMR spectrum. Biological tissues have a wide range of domain orientations, and a range of EFG and η values. Therefore, a Gaussian distribution of ω_Q is assumed for such poorly ordered systems. Within this model, the equations for the sodium MQF-NMR signals have to be appropriately weighted by a Gaussian distribution of ω_Q as given by the function:

$$W(\omega_Q) = \frac{1}{\sqrt{2\pi}\sigma}e^{-(\omega_Q - \bar{\omega}_Q)^2/2\sigma^2} \qquad (5)$$

The Gaussian distribution is centered on zero, i.e., the mean of the quadrupolar interaction frequencies, $\bar{\omega}_Q$ = 0 and σ is defined as the RMS of ω_Q values over all domains.

In this study, we are particularly interested in the double-quantum filtered magic angle (DQFMA), triple-quantum filtered (TQF) signals. The DQFMA signal is generated by sodium in purely anisotropic environments, whereas the TQF signal originates primarily from sodium in isotropic slow motion environments (9,25,26). The real part of the TQF signal from a spin-3/2 system with a static Gaussian distribution of ω_Q is given by:

$$S(t > \tau) = -\frac{9}{40\sqrt{2}}\left[\exp(-s_2 t) + \frac{1}{2}\exp(-s_1 t)\exp\left(-\frac{\sigma^2 t^2}{2}\right) - \exp(-s_1 t)\exp(-s_2(t-\tau))\exp\left(-\frac{\sigma^2 t^2}{2}\right) - \exp(-s_2 t)\exp(-s_1(t-\tau))\exp\left(-\frac{\sigma^2(t-\tau)^2}{2}\right) + \frac{1}{2}\left[\exp(-s_1 t) - \exp\left(-\frac{\sigma^2(t-2\tau)^2}{2}\right)\right]\right] \quad (6)$$

The corresponding DQFMA signal is:

$$S(t > \tau) = \frac{1}{5\sqrt{2}} \cdot \exp(-s_1 t)\left[\exp\left(-\frac{\sigma^2 t^2}{2}\right) - \exp\left(-\frac{\sigma^2(t-2\tau)^2}{2}\right)\right] \quad (7)$$

Where t is the detection time (begins immediately after the first pulse), τ is the preparation time, and the variables s_1 and s_2 are the transverse relaxation rate constants, $1/T_{2f}$ and $1/T_{2s}$, respectively. Equations [6] and [7] were used to fit the sodium MQF-NMR signal obtained experimentally. The fits were used to determine σ and the relaxation time constants, T_{2s} and T_{2f}.

METHODS

Sample Preparation

Samples of bovine articular cartilage were obtained from a local slaughterhouse (Bierig Bros., Vineland, NJ) within 3 hours after slaughter. Using a sterile cork borer, 15 8-mm-diameter, cylindrical cartilage plugs were cored from the same region in 15 different patellae. IL-1β treatment was based on a previously described technique (27). All chemical compounds were obtained from GIBCO BRL (Gaithersburg, MD) unless otherwise indicated. Samples were washed in phosphate-buffered saline (PBS) (Sigma Chemicals, St. Louis, MO) containing 100 units/mL penicillin/streptomycin, 0.25 μg/mL amphotericine B, and 1 mM hepes. The samples were separated into three groups of five plugs and each group was placed into sterile six-well culture plates for 24 hours. These plates contained Dulbecco's Modified Eagle's Medium (DMEM) with 10 μg/mL of insulin, 10 μg/mL of transferrin, 100 units/mL of penicillin, 100 μg/mL of streptomycin, 0.25 μg/mL amphotericine B, 2 mM L-glutamine, and 50 μg/mL ascorbic acid (Sigma Chemicals, St. Louis, MO). After equilibration, the medium was removed and the cartilage plugs were placed in fresh medium. Three plugs from each group were subjected to a solution of DMEM containing 20 ng/mL of IL-1β (Sigma, St. Louis, MO), while the other two samples were placed in normal DMEM solution to serve as controls. The medium was refreshed every 3 days. Samples from the first group were removed from culture after 4 days for NMR measurements. Likewise, the second and third groups were removed from culture after 6 and 7 days, respectively, and the NMR experiments were performed. In this way, samples with different degrees of PG loss were obtained. Media from each sample were saved for further analysis to determine PG loss from the plugs in culture. The samples were placed in a sealed tube for the NMR experiments to avoid dehydration. The position of the cartilage plug inside the magnet was such that the normal to the articular surface was perpendicular to the static magnetic field, B_0.

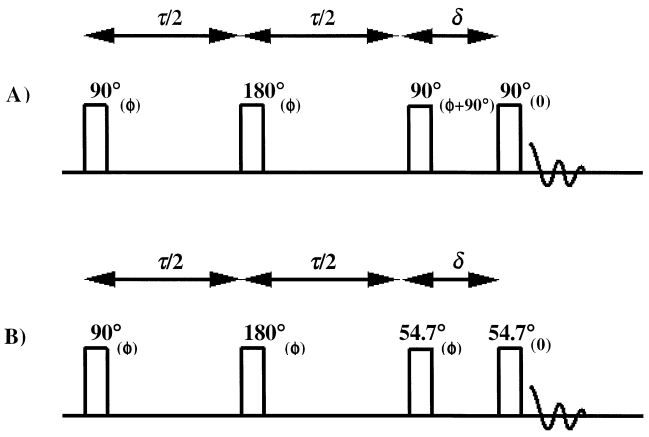

Figure 1. MQF-NMR pulse sequence for obtaining (**A**) TQF and (**B**) DQFMA spectra. The RF pulses were phase-cycled with six RF phases (ϕ = 30°, 90°, 150°, 210°, 270°, and 330°) for the TQF sequence and four times (ϕ = 0°, 90°, 180°, and 270°) for the DQFMA sequence.

NMR Measurements

All NMR experiments were performed on a 2T whole-body Oxford magnet attached to a custom-built pulse-programming computer interface. A seven-turn, 1-cm-diameter solenoid coil tuned to ^{23}Na at 2T (22.7 MHz) was used to obtain all sodium NMR spectra. Single quantum spectra were obtained with a standard pulse-acquisition sequence. A typical 90° pulse length was 25 μs. Sodium T_1 was measured from spectra obtained with a standard inversion recovery (IR) sequence with 20 inversion times ranging from 2 to 40 msec. Multiple-quantum filtering was performed using pulse sequences described by Reddy et al (28). Sodium TQF spectra were used to determine T_{2s}, and DQFMA spectra were employed to calculate T_{2f} and σ.

TQF spectra were obtained with the pulse sequence shown in Figure 1A. The pulse sequence consists of four radiofrequency (RF) pulses. The first pulse is a 90° pulse, which produces single-quantum coherence. It is followed by a 180° refocusing pulse after a time $\tau/2$ (half the preparation time). During the preparation time, the magnetization evolves in the presence of quadrupolar relaxation as well as the RQI (15). Two more 90° pulses separated by a time δ (evolution time) are applied another $\tau/2$ period after the refocusing pulse. The first of these two pulses creates multiple-quantum coherences (triple-quantum in this case), which are then converted by the second pulse to odd-ranked tensors ($T^1_{\pm 1}$, $T^3_{\pm 1}$), which evolve into the observable single-quantum signal

($T^1_{\pm1}$). The RF pulses were phase-cycled with six RF phases (ϕ = 30°, 90°, 150°, 210°, 270°, and 330°) while the acquisition phase was alternated between 0° and 180°. The six phase-cycled signals were then combined to obtain one TQF spectrum. In the measurement of relaxation times the τ time was varied 18 times from 0.4 to 35 msec and the δ time was kept as small as possible (400 μs). Each spectrum was averaged 100 times to enhance the signal-to-noise ratio (SNR). The pulse sequence repetition time (TR) was 100 msec, so the total acquisition time was 18 minutes for each sample.

DQFMA spectra were obtained with the pulse sequence shown in Figure 1B. It is similar to the TQF pulse sequence except that the last two pulse flip angles are set to 54.7°. In this sequence, only the double-quantum coherence due to even-rank tensor ($T^2_{\pm2}$) will be detected. This coherence purely arises from the presence of RQI. The RF pulses were phase-cycled with four RF phases (ϕ = 0°, 90°, 180°, and 270°). Spectra were obtained by varying the preparation time from 0.2 to 10 msec in 15 steps, while the evolution time was fixed at 400 μs. As with the TQF pulse sequence, the acquisition phase was alternated between 0° and 180°. Each DQFMA spectrum was averaged 300 times. The TR time was 100 msec for the DQFMA sequence, resulting in a total acquisition time of 30 minutes per sample.

PG Assay

After the NMR experiments, the amount of PG depleted from each plug was determined by subjecting the degradation media of each plug to a dimethylmethylene blue (DMMB) spectrophotometric assay (29). To determine the total PG content, the entire cartilage plug was digested with 500 μg/mL of papain for 24 hours after the NMR experiments. A solution of DMMB was prepared by mixing 8 mg of DMMB in 496.5 mL of water containing 1 g of sodium formate, 2.5 mL ethanol, and 1 mL formic acid (pH = 3.6 and A_{535} = 0.47). Absorbances at 535-nm wavelength were obtained with a Spectronic 20D+ spectrophotometer (Spectronic Instruments, Rochester, NY). Calibration was performed using 0–30 μl of 1 mg/mL of chondroitin sulfate C (Sigma Chemicals, St. Louis, MO) with additional PBS to make up 50 μl in a 4.5-mL methacrylate cuvette. Two mL of the DMMB solution were added to each standard and the % transmittance was read immediately. The standard curve was plotted using the absorbance of each standard (calculated from the % transmittance by Beer's Law). Reagent blanks were used to recalibrate the spectrophotometer before each set of samples was read. Samples of 10 μl of the degradation media (and 2 μl of the papain digested media) with additional PBS to make up 50 μl were created. Two mL of the DMMB solution were added to each of the unknowns, and the transmittance was read. The amount of PG was determined from the absorbance and the standard curve. The total PG from each sample was determined by adding the PG in the degradation medium and the PG in the corresponding cartilage plug (obtained by digestion with papain).

Collagen Assay

To determine the effect of IL-1β degradation on collagen content in cartilage, in a separate experiment another nine cartilage plugs were cultured in the exact same way as the original 15 plugs. Then the cultured media and the papain digests were subjected to both PG assay (as described above) and collagen assay. Commonwealth Biotechnologies Inc. (Richmond, VA) performed the collagen assays in the following way. Two hundred μl of each sample were transferred to a pyrolyzed glass tube. The samples were taken to dryness and hydrolyzed in 1 mL of 6N HCl for 20 hours at 110°C. Following hydrolysis, the samples were again taken to dryness and dissolved in 200 μl of sample loading buffer. The amino acid content of each sample was then analyzed via chromatograms.

Histology

Histology was performed on three controls and three samples treated with IL-1β. Each cartilage plug was fixed with 10% formalin, decalcified for 2 days, and embedded in paraffin wax. A microtome (Microm, Germany) was used to slice 5-μm-thick sections across cartilage. Histology sections were mounted on slides and stained with Safranin-O (Sigma, St. Louis, MO) with a Fast Green counterstain to distinguish normal and PG-depleted cartilage tissue, respectively. The slides were examined under an SV11 stereo microscope (Carl Zeiss Inc., Thornwood, NY) and images were captured into the computer using SCION Image software (Scion Corp., Frederick, MD).

Data Processing

NMR spectra were processed using spectral-processing routines written in IDL (RSI, Boulder, CO) data processing language. An exponential-weighted filter to smooth the data was applied to the raw free induction decay signals. Then the corresponding spectrum was obtained by a Fourier transform. A graphical-user-interface-based program was written in IDL to fit DQFMA and TQF spectra. Spectra for each τ time were phased and then fitted to the Fourier transform of either Eq. [6] or [7] using a nonlinear, Levenberg-Marquardt-based algorithm. Statistical analysis was performed with the JMP software package (SAS Institute, Cary, NC) to determine the *P*-values of the correlation coefficients (R^2) between the observed values and the values predicted by the model.

The DQFMA spectra were used to calculate sodium T_{2f} and σ. The T_{2f} and σ values for each plug were obtained by averaging the T_{2f} and σ obtained by fitting the eight spectra (of the 15 spectra per plug) with the highest SNR. With these two numbers as input, the TQF spectra were used to calculate sodium T_{2s}. The T_{2s} for a plug was obtained by averaging the T_{2s} of the 10 (of 18 spectra) highest-amplitude spectra.

Sodium T_1 was calculated by fitting the IR spectral amplitudes ($S(TI)$) as a function of inversion time (TI) to the equation:

$$S(TI) = S_o(1 - 2e^{-TI/T_1}) + C \qquad (8)$$

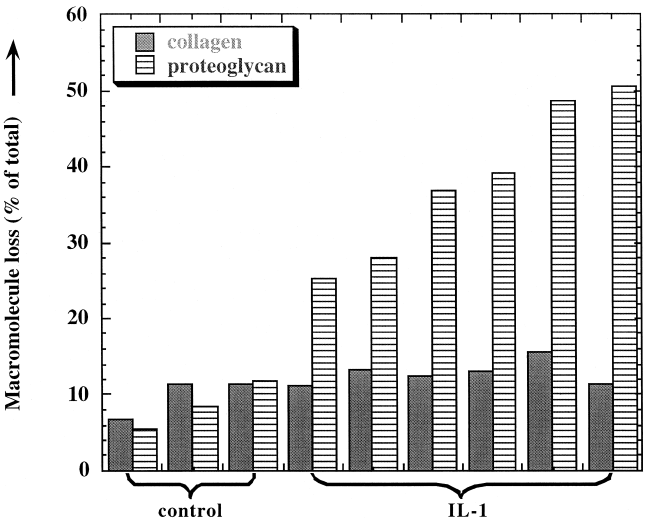

Figure 2. Changes in collagen and proteoglycan (PG) content in bovine articular cartilage specimens treated with IL-1β.

Where S_o is the signal intensity of the equilibrium magnetization and C is the baseline offset. A nonlinear, least-squares algorithm was used to determine the best fit.

RESULTS

Although IL-1β-induced macromolecular degradation resulted in a loss of collagen, we found that the percentage of collagen lost (as measured by collagen assay) was significantly less than the percentage of PG loss (as measured by PG assay) from each plug (Fig. 2). Furthermore, there is no significant change in the amount of collagen loss as a function of concentration of IL-1β used in our degradation method. However, we clearly observed an increased PG loss with increasing IL-1β degradation. As a result, the sodium NMR parameters (T_{2s}, T_{2f}, T_1, and σ) are plotted as functions of PG loss by the specimen and not the percentage of collagen loss in the subsequent graphs.

Figure 3 shows typical sodium TQF spectra (dotted line) and fit (solid line) obtained at τ = 5 msec from bovine articular cartilage plugs degraded with IL-1β. The corresponding DQFMA spectra for τ = 800 μs for the same two specimens are shown in Figure 4. The fits were obtained with Eqs. [6] and [7]. The control specimen in A lost 6% of its total PG (probably from autodigestion of PG) resulting in σ = 177 Hz, T_{2f} = 3.35 msec, and T_{2s} = 12.7 msec, as calculated from the fits. The IL-1β-degraded specimen in B lost more than half of its total PG; σ = 120 Hz, T_{2f} = 2.48 msec, and T_{2s} = 14.8 msec were the parameters for the fits. The TQF spectra are normalized to their corresponding single-quantum integrated spectral areas.

The difference between the two samples is more obvious when we plot the spectral amplitudes as a function of preparation time, τ (Fig. 5). The DQFMA spectral amplitudes (A) for the IL-1β-degraded specimen reach a minimum value at τ = 1.2 msec, whereas for the control sample the minimum is reached 400 μs later. The longer T_{2s} for the IL-1β-degraded sample is evident by the slower decay of its TQF spectral amplitudes (B).

Histological sections from a control and an IL-1β-degraded specimen are shown in Figure 6. Normal cartilage (with higher PG content) appears red, whereas PG-depleted cartilage is blue with the staining used in this study. The slides illustrate that PG loss is nonuniform across the cartilage. There is more loss at the

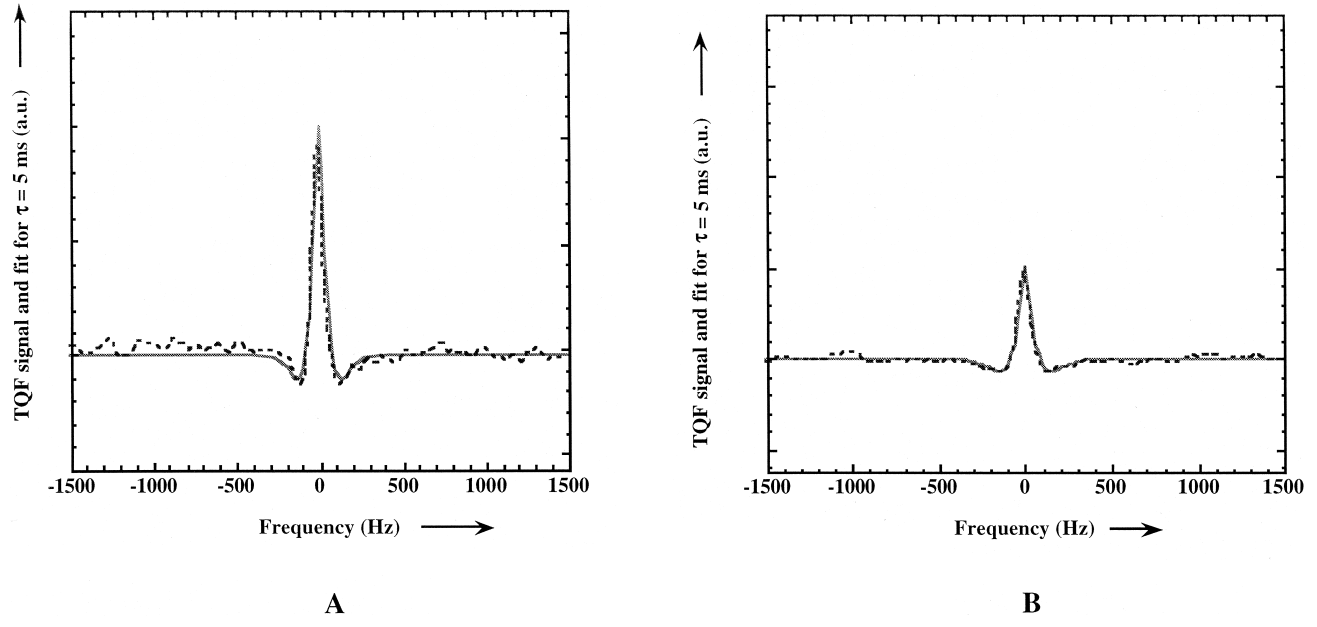

Figure 3. Sodium TQF spectra (dotted line) and fits (solid line) from two IL-1β-degraded bovine articular cartilage specimens. Each spectrum is normalized by its single-quantum spectrum. Total PG lost was (**A**) 6% from a control specimen and (**B**) 52% from an IL-1β-degraded specimen. Preparation time = 5 msec for both spectra. The mean square difference between the fit and the data was less than 1×10^{-4} for both fits.

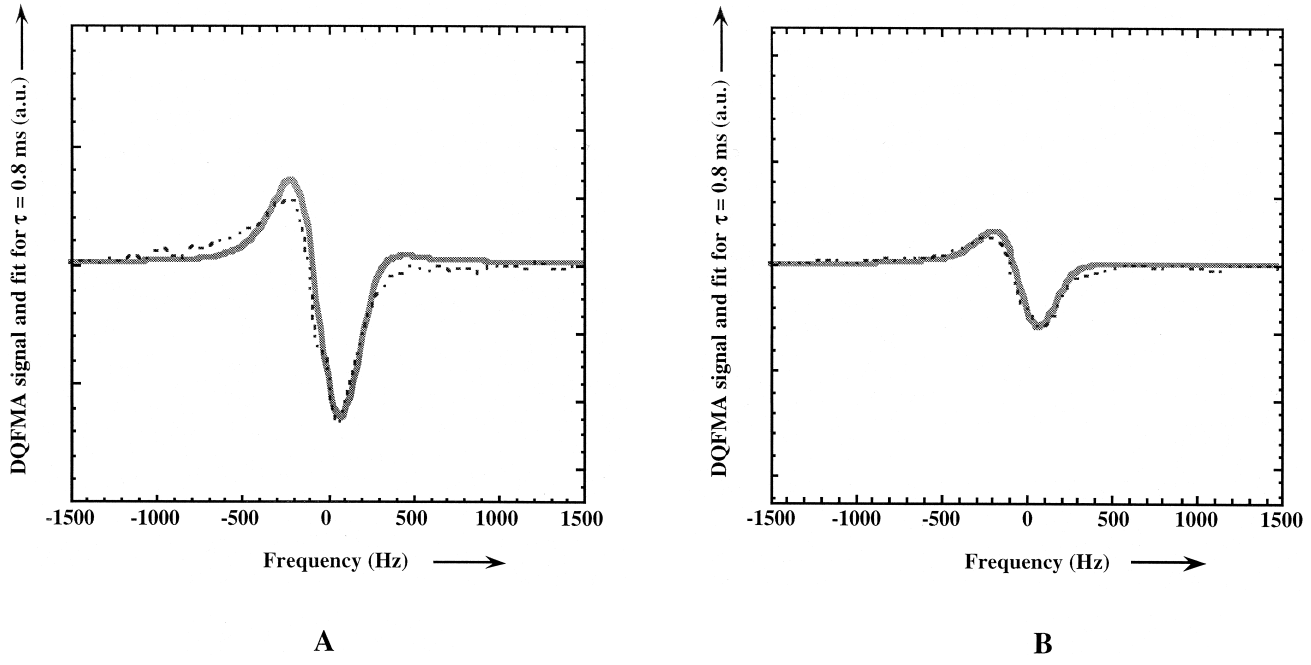

Figure 4. The DQFMA spectra (dotted line) and fits (solid line) for the same cartilage specimens from Figure 3. Preparation time (τ) = 800 μs for both spectra. The mean square difference between the fit and data for both plots was less than 1×10^{-4}.

articular and chondral surfaces and less PG loss in the middle of the tissue.

The variation in relaxation times as a function of PG loss from the cartilage plugs is shown in Figure 7. A spectrophotometric assay to determine PG content was performed only on nine specimens. The other six samples were used for histology. The first three data points (corresponding to a PG loss of 6%, 6%, and 8%) are all control specimens. The PG loss in the controls is a result of autodigestion of cartilage macromolecules while in the culture medium. Figure 7 shows that there is a significant increase in T_1 with PG loss ($P < 0.01$). T_1 ranged from 16 msec for a 6% PG loss to 21 msec for a 52% PG loss. T_{2s} was 12.3 msec for a 6% PG-depleted specimen and increased with PG depletion, resulting in a time of 14.9 msec for the specimen with 50% PG loss. Statistical analysis determined this trend to be significant ($P < 0.01$). The short component of the transverse relaxation time, T_{2f}, decreases significantly ($P < 0.01$) with increasing PG depletion (Fig. 8). The longest T_{2f}

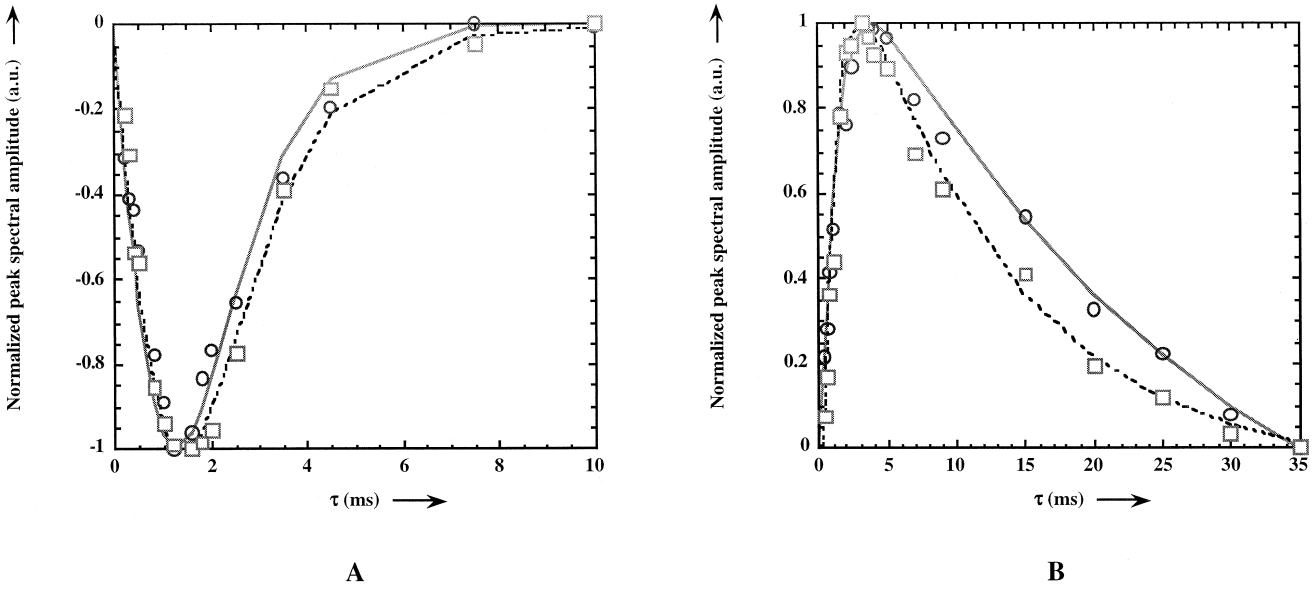

Figure 5. Normalized DQFMA (**A**) and TQF (**B**) spectral amplitudes versus preparation time for the control (□, dotted line-fit) and IL-1β degraded (○, solid line-fit) specimens from Figure 3. The relative differences in the relaxation rates and ω_Q between these two specimens are evident in these graphs.

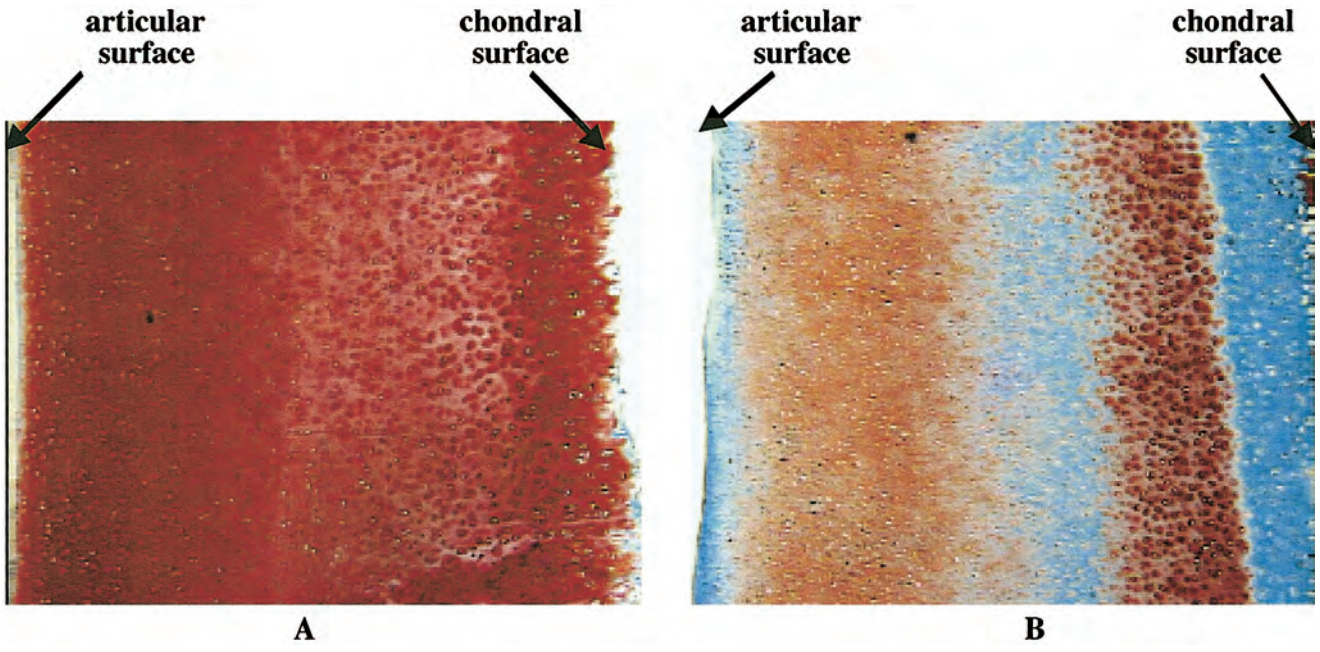

Figure 6. Histology sections from (**A**) a control and (**B**) an IL-1β-degraded specimen of bovine articular cartilage. The red represents PG-abundant regions, and blue indicates a loss of PG. The PG loss is nonuniform across the cartilage, with more loss at the articular and chondral surfaces and less in the middle of the tissue.

was 3.50 msec for the 8% PG loss specimen and decreased to 2.26 msec for the specimen with 50% PG loss. As explained in the Data Processing section, for every plug σ, T_{2f}, and T_{2s} values were obtained by averaging these parameters from several fits of spectra obtained at different τ times. Measurements of relative error of the fitting procedures, which can be obtained from the standard deviations of these values, were less than 5% of their average value in each plug.

Figure 9 plots σ as a function of PG loss by the specimen. The quadrupolar interaction frequency remains fairly constant until a 25% loss of PG. Beyond this point, σ decreases by approximately 20% with increasing PG loss. Therefore, there is a substantial decrease in order with PG loss.

DISCUSSION

It was previously shown (15) that collagen alone is responsible for σ changes in cartilage. This was determined from the fact that a collagen suspension produced a DQF spectrum, whereas a suspension of PG did not. This may be the case for isolated ECM constituents. However, as shown here in intact cartilage, PG

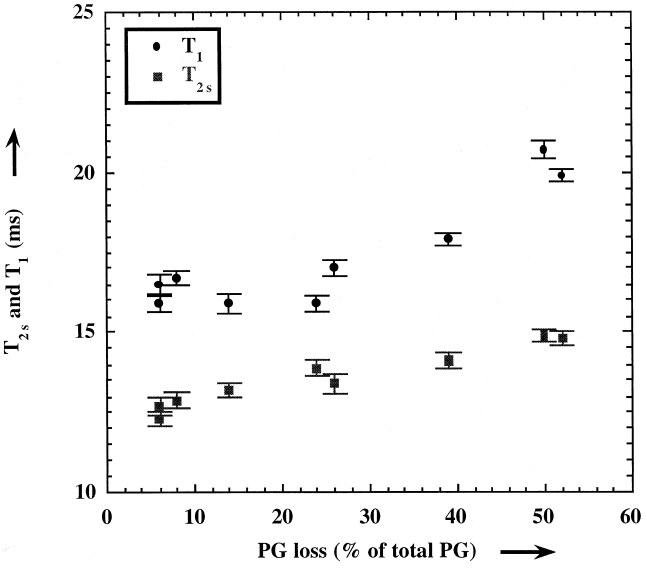

Figure 7. Plot of T_{2s} (■) and T_1 (●) as a function of the PG lost by the sample. Only the data from the nine specimens that were subjected to a PG assay are shown.

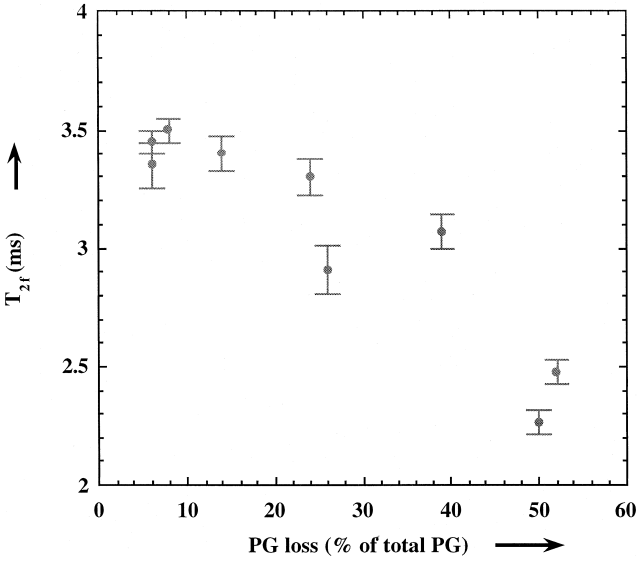

Figure 8. Plot of T_{2f} as a function of the PG lost by the sample.

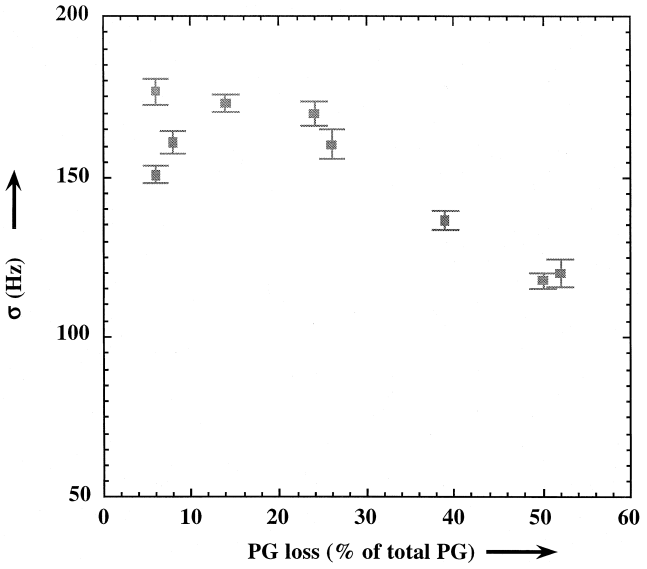

Figure 9. Plot of the RMS RQI frequency, σ, as a function of PG loss by the sample.

loss also leads to change in the quadrupolar coupling constant, and hence the order of macromolecules in the tissue. This may be due to a decrease in the repulsive forces between negatively charged PG molecules in cartilage that influence the orientation of the collagen fibrils. Therefore, in intact cartilage, it is possible that the PG loss may be affecting the order either by influencing the collagen ordering or by changing the organization of both collagen and PG.

In conclusion, we have shown that in intact cartilage, cytokine-induced degradation changes not only sodium relaxation characteristics but also ω_Q, and hence the order of macromolecules in the tissue. The results showed that T_{2f} decreased whereas T_{2s} and T_1 increased with increasing PG loss from cartilage. There was a significant decrease in order (σ) with PG loss. Contrary to the results obtained from isolated model systems of ECM of cartilage, in intact cartilage PG also contributes to the ω_Q and hence the order of macromolecules in the tissue. These results also demonstrate that MQF spectroscopy is uniquely suited for determining the macromolecular order in tissues in a nondestructive fashion. This measurement provides indirect information about structural changes in the tissue in response to artificially induced or natural pathology. To the best of our knowledge, no other method provides this information in a noninvasive, nondestructive manner. In conjunction with currently available MQF-MRI techniques, it should be possible to quantify changes in sodium MR parameters in cartilage pathology in vivo.

ACKNOWLEDGMENTS

We thank Professor John S. Leigh for his encouragement and support.

REFERENCES

1. Mankin HJ, Dorfman H, Zarins L. Biochemical and metabolic abnormalities in articular cartilage from osteoarthritic human hips. II. Correlation of morphology with biochemical and metabolic data. J Bone Joint Surg 1971;53A:523–537.
2. van de Loo AA, Arntz OJ, Otterness IG, van den Berg WB. Proteoglycan loss and subsequent replenishment in articular cartilage after a mild arthritic insult by IL-1 in mice: impaired proteoglycan turnover in the recovery phase. Agents Actions 1994; 41:200–208.
3. Maroudas A, Muir H, Wingham J. The correlation of fixed negative charge with glycosaminoglycan content of human articular cartilage. Biochim Biophys Acta 1969;177:492–500.
4. Lesperance LM, Gray ML, Burstein D. Determination of fixed charge-density in cartilage using nuclear-magnetic-resonance. J Orthop Res 1992;10:1–13.
5. Jelicks LA, Paul PK, O'Byrne E, Gupta RK. H-1, Na-23, and C-13 MR spectroscopy of cartilage degradation in vitro. J Magn Reson Imaging 1993;3:565–568.
6. Reddy R, Insko EK, Noyszewski EA, Dandora R, Kneeland JB, Leigh JS. Sodium MRI of human articular cartilage *in vivo*. Magn Reson Med 1998;39:697–701.
7. Shapiro EM, Borthakur A, Dandora R, Kriss A, Leigh JS, Reddy R. Sodium visibility and quantitation in intact bovine articular cartilage using high field 23Na MRI and MRS. J Magn Reson 2000;142: 24–31.
8. Pekar J, Leigh JS. Detection of bi-exponential relaxation in sodium-23 facilitated by double quantum filtering. J Magn Reson 1986; 69:582–584.
9. Eliav U, Shinnar H, Navon G. The formation of second rank tensor in 23Na double-quantum-filtered NMR as an indicator for order in biological tissues. J Magn Reson 1992;98:223–229.
10. Reddy R, Bolinger L, Shinnar M, Noyszewski EA, Leigh JS. Detection of residual quadrupolar interaction in human skeletal muscle and brain *in vivo* via multiple quantum filtered sodium NMR spectra. Magn Reson Med 1995;33:134–139.
11. Reddy R, Li SC, Noyszewski EA, Kneeland JB, Leigh JS. *In vivo* sodium multiple quantum spectroscopy of human articular cartilage. Magn Reson Med 1997;38:207–214.
12. Borthakur A, Hancu I, Boada FE, Shen GX, Shapiro EM, Reddy R. *In vivo* triple quantum filtered twisted projection sodium MRI of human articular cartilage. J Magn Reson 1999;141:286–290.
13. Shinar H, Knubovets T, Eliav U, Navon G. Sodium interaction with ordered structures in mammalian red blood cells detected by Na-23 double quantum NMR. Biophys J 1993;64:1273–1279.
14. Springer CS. Biological systems: spin-3/2 nuclei. In: Grant DM, Harris RK, editors. Encyclopedia of nuclear magnetic resonance. New York: John Wiley and Sons; 1996. p 940–951.
15. Eliav U, Navon G. Analysis of double-quantum-filtered NMR spectra of 23Na in biological tissues. J Magn Reson 1994;B103: 19–29.
16. Towle CA, Hung HH, Bonassar LJ, Treadwell BV, Mangham DC. Detection of interleukin-1 in the cartilage of patients with osteoarthritis: a possible autocrine/paracrine role in pathogenesis. Osteoarthritis Cartilage 1997;5:293–300.
17. Venn G, Nietfeld JJ, Duits AJ, et al. Elevated synovial fluid levels of interleukin-6 and tumor necrosis factor associated with early experimental canine osteoarthritis. Arthritis Rheum 1993;36:819–826.
18. Tyler JA. Cartilage degradation. In: Hall BK, Newman S, editors. Cartilage: molecular aspects. Boca Raton, FL: CRC Press; 1991. p 213–256.
19. Hardingham TE, Bayliss MT, Rayan V, Noble DP. Effects of growth factors and cytokines on proteoglycan turnover in articular cartilage. Br J Rheumatol 1992;31:1–6.
20. Tyler JA, Benton HP. Synthesis of type II collagen is decreased in cartilage cultured with interleukin 1 while the rate of intracellular degradation remains unchanged. Coll Relat Res 1988;8: 393–405.
21. Bashir A, Gray ML, Burstein D. Sodium T_1 and T_2 in control and degraded cartilage: implications for determination of tissue proteoglycan content. In: Proceedings of the 3rd Annual Meeting of SMR, 1995. p 1896.
22. Kemp-Harper R, Wickstead B, Wimperis S. Sodium ions in ordered environments in biological systems: analysis of 23Na NMR spectra. J Magn Reson 1999;140:351–362.
23. Woessner DE, Bansal N. Temporal characteristics of NMR signals from spin 3/2 nuclei of incompletely disordered systems. J Magn Reson 1998;133:21–35.

24. Hancu I, Boada FE, Shen GX. Three-dimensional triple-quantum-filtered 23Na imaging of *in vivo* human brain. Magn Reson Med 1999;42:1146–1154.
25. Jaccard G, Wimperis S, Bodenhausen G. Multiple quantum NMR spectroscopy of S=3/2 spins in isotropic phase: a new probe for multiexponential relaxation. J Chem Phys 1986;85:6282–6293.
26. van der Maarel JRC. Relaxation of spin 3/2 in a non-zero average electric field gradient. Chem Phys Lett 1989;155:288–296.
27. Loulakis P, Shrikhande A, Davis G, Maniglia CA. N-terminal sequence of proteoglycan fragments isolated from medium of interleukin-1-treated articular-cartilage cultures. Putative site(s) of enzymic cleavage. Biochem J 1992;284:589–593.
28. Reddy R, Insko EK, Leigh JS. Triple quantum sodium imaging of articular cartilage. Magn Reson Med 1997;38:279–284.
29. Farndale RW, Sayers CA, Barrett AJ. A direct spectrophotometric microassay for sulfated glycosaminoglycans in cartilage cultures. Connect Tiss Res 1982;9:247–248.